

# JOURNAL

## OF THE AMERICAN CHEMICAL SOCIETY

Registered in U.S. Patent Office. © Copyright, 1981, by the American Chemical Society.

VOLUME 103, NUMBER 22

NOVEMBER 4, 1981

### Nuclear Quadrupole Coupling Constants and Hydrogen Bonding. A Molecular Orbital Study of Oxygen-17 and Deuterium Field Gradients in Formaldehyde–Water Hydrogen Bonding

Leslie G. Butler and Theodore L. Brown\*

Contribution from the School of Chemical Sciences and Materials Research Laboratory, University of Illinois, Urbana, Illinois 61801. Received February 23, 1981

**Abstract:** A model hydrogen-bond system consisting of formaldehyde and water molecules has been studied by "ab initio" molecular orbital (MO) methods, using a "near-double-zeta" basis set. Quadrupole coupling constants have been calculated for the carbonyl oxygen, the water oxygen, and the hydrogen-bonded deuterium site as a function of the hydrogen-bond geometry. Strong hydrogen-bond formation results in a decrease in the  $^{17}\text{O}$  nuclear quadrupole coupling constant of about 2.5 MHz with respect to the non-hydrogen-bonded molecules for both the carbonyl and water oxygen sites. The origins of the decrease are discussed, and comparisons are drawn with experimental  $^{17}\text{O}$  NQR data. The calculated deuterium quadrupole coupling constant decreases dramatically with decreasing O...O distance in agreement with available experimental data. The possibility of a negative sign for the  $^2\text{H}$  quadrupole coupling constant in short, symmetric hydrogen bonds is considered. It seems unlikely that the  $^2\text{H}$  quadrupole coupling constant is negative in sign for any known O—H...O hydrogen bond.

#### Introduction

The central importance of hydrogen bonding in determining the properties of many substances, as well as its role in biological systems, has led to a rich literature.<sup>1-3</sup> Numerous experimental techniques, including X-ray and neutron diffraction, infrared spectroscopy, and nuclear magnetic resonance spectroscopy, have been applied to the study of hydrogen bonding in solids. Because of experimental difficulties, nuclear quadrupole resonance (NQR) spectroscopy has not been so widely employed. It is, however, potentially a very valuable tool, because the electric field gradient at a nucleus such as  $^2\text{H}$ ,  $^{14}\text{N}$ , or  $^{17}\text{O}$ , on which the NQR spectrum depends, is the expectation value of a one-electron operator.<sup>4</sup> This means that the value of the operator is determined by the ground-state charge distribution. The NQR spectra thus relate to details of the electronic and nuclear charge distribution about the nucleus of interest. When the geometrical configuration is known from a diffraction study, the NQR data can be employed to extract insights into the electronic charge distribution. It is from these details of charge distribution that one learns more about how hydrogen bonding affects structure and chemical reactivity.

Recent advances in double resonance methods for obtaining NQR spectra have opened up new possibilities for using NQR

as a probe of hydrogen bonding.<sup>5-7</sup> We have embarked on an experimental program which involves measurements of the NQR spectra of  $^2\text{H}$ ,  $^{14}\text{N}$ , and  $^{17}\text{O}$  in hydrogen-bonded systems. This first paper deals with a theoretical treatment of a simple hydrogen-bonding system, involving formaldehyde and water. It was chosen for study as a simple prototype of an important class of hydrogen-bonding interactions, between an O—H function and a singly connected carbonyl-type oxygen. The field gradients at the deuterium in the hydrogen bond and at both oxygen atoms have been evaluated for a range of geometries. In the case of deuterium, a substantial body of prior experimental evidence has pointed to the existence of a useful correlation between coupling constant at deuterium in the A—H...B system, and the A—H or A...B distances.<sup>8-14</sup> Work in our laboratories has shown that the field gradient at  $^{17}\text{O}$  in singly connected oxygen is substantially affected also by the presence of hydrogen bonding.<sup>15</sup> We have compared the results of the molecular orbital calculations with these currently available experimental data.<sup>72</sup>

(1) Pimentel, G. C.; McClellan, A. L. "The Hydrogen Bond"; W. H. Freeman: San Francisco, 1960.

(2) Hamilton, W. C.; Ibers, J. A. "Hydrogen Bonding in Solids"; W. A. Benjamin: New York, 1968.

(3) Schuster, P.; Zundel, G.; Sandorf, C., Eds. "The Hydrogen Bond"; North-Holland Publishing Co.: Amsterdam, 1976; Vols 1-3.

(4) Lucken, E. A. C. "Nuclear Quadrupole Coupling Constants"; Academic Press: London, 1969.

(5) Edmonds, D. T. *Phys. Rep. C* **1977**, *29*, 233.

(6) Rubenacker, G. V.; Brown, T. L. *Inorg. Chem.* **1980**, *19*, 392.

(7) Cheng, C. P.; Brown, T. L. *Symp. Faraday Soc.* **1979**, No. 13, 75.

(8) Chiba, T. *J. Chem. Phys.* **1964**, *41*, 1352.

(9) Soda, G.; Chiba, T. *J. Phys. Soc. Jpn.* **1969**, *26*, 249.

(10) Soda, G.; Chiba, T. *J. Chem. Phys.* **1969**, *50*, 439.

(11) Goren, S. D. *J. Chem. Phys.* **1974**, *60*, 1892.

(12) Hunt, M. J.; Mackay, A. L. *J. Magn. Reson.* **1974**, *15*, 402.

(13) Berglund, B.; Vaughan, R. W. *J. Chem. Phys.* **1980**, *75*, 2037.

(14) Berglund, B.; Lindgren, J.; Tegenfeldt, J. J. *Mol. Struct.* **1978**, *43*, 179.

(15) Cheng, C. P.; Brown, T. L. *J. Am. Chem. Soc.* **1979**, *101*, 2327.

Table I. Comparison of Calculated and Observed Quadrupole Coupling Constant and Asymmetry Parameters for the Separated Formaldehyde and Water Molecules

	basis set	[3s2p/2s]	[4s2p/2s]	[5s3p2d/2slp]	exptl <sup>a</sup>	ref
H <sub>2</sub> C <sup>17</sup> O	$e^2Qq_{zz}/h$ (MHz)	15.733	15.726 <sup>b</sup>	13.668 <sup>c</sup>	12.37 (1)	32
	$\eta$	0.467	0.467	0.644	0.697 (3)	
H <sub>2</sub> <sup>17</sup> O	$e^2Qq_{zz}/h$ (MHz)	12.544	12.333 <sup>b</sup>	11.467 <sup>d</sup>	10.175 (67)	41
	$\eta$	0.793	0.766	0.823	0.75 (1)	
DHO	$e^2Qq_{zz}/h$ (kHz)	383.5	377.1 <sup>b</sup>	356.8 <sup>d</sup>	318.6 (2.4)	54
	$\eta$	0.115	0.116	0.134	0.06 (.16)	

<sup>a</sup> Uncertainty in parentheses. <sup>b</sup> Calculated from the values given in ref 23. <sup>c</sup> Recalculated from the values given in ref 62 using current values of  $Q$ . <sup>d</sup> Recalculated from the values given in ref 22 using current values of  $Q$ .

### Theory

In pure NQR spectroscopy transitions are observed between energy levels determined by the quadrupolar Hamiltonian,  $H_Q$ :<sup>16</sup>

$$H_Q = \frac{e^2Qq_{zz}}{4S(2S-1)} \left[ 3S_z^2 - S^2 + \frac{\eta}{2}(S_+^2 + S_-^2) \right] \quad (1)$$

The quantity  $e^2Qq_{zz}/h$  is termed the quadrupole coupling constant,  $S$  is the nuclear spin, and  $\eta$  is the asymmetry parameter. The nuclear quadrupole moments  $Q$  for deuterium<sup>17</sup> and oxygen-17<sup>18</sup> are  $+2.860 \times 10^{-27}$  and  $-2.562 \times 10^{-26}$  cm<sup>2</sup>, respectively. The electric field gradient (efg),  $q$ , is a traceless second-order tensor. It is diagonal in a principal axis system ( $X, Y, Z$ ) which by convention is chosen so that  $|q_{zz}| > |q_{yy}| > |q_{xx}|$ . The asymmetry parameter, defined as  $\eta = (q_{xx} - q_{yy})/q_{zz}$ , varies between 0 and 1. The asymmetry parameter and  $q_{zz}$  are normally employed to express the two independent components of the efg tensor.

The efg at a given nucleus is the sum of electronic and nuclear contributions. Thus, for example,  $q_{zz}$  is expressed as

$$eq_{zz} = e \sum K_n \frac{3Z_n^2 - r_n^2}{r_n^5} - e \left\langle \Psi^* \left| \sum \frac{3Z_i^2 - r_i^2}{r_i^5} \right| \Psi \right\rangle \quad (2)$$

where  $e$  is the electronic charge, the index  $n$  is taken over all other nuclei, of charges,  $K_n$ , and  $i$  is taken over all electrons. Analogous expressions apply for  $eq_{xx}$  and  $eq_{yy}$ . As indicated earlier,  $q_{zz}$  is the expectation value of a one-electron operator. The wave function  $\Psi$  represents the ground-state wave function.

Methods for evaluating eq 2 for Gaussian<sup>19</sup> and Slater-type orbitals<sup>20</sup> have been given. Because the field gradient operator contains a  $r^{-3}$  dependence, its calculated value is very sensitive to the behavior of the wave function in the near vicinity of the nucleus. It is thus important to employ a good quality wave function if one is to obtain reasonable results for the field gradient operator. We have employed the "near-double-zeta" Gaussian basis set of Dunning and Hay (9s5p/4s),<sup>21</sup> contracted to (3s2p/2s). The elements of the efg tensor were calculated for the molecular orbital coefficient matrix, using a program originally written by Moskowitz,<sup>22</sup> and modified by W. C. Ermler. The geometries of the formaldehyde and water molecules were chosen to correspond to those employed by Snyder and Basch.<sup>23</sup>

The most thoroughly studied geometrical arrangement is the syn form, shown in Figure 1. The ground-state wave functions

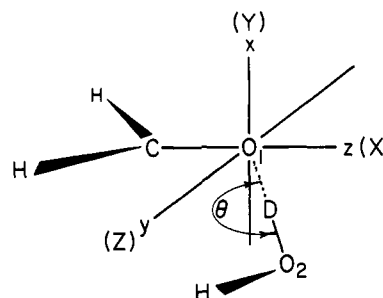


Figure 1. Geometrical arrangement employed in calculations on the formaldehyde-water hydrogen-bond interaction. The  $O_1 \cdots O_2$  distance was varied in the range 3.2 to 2.4 Å. The C-O<sub>1</sub>-D angle was in all cases 120°. In the general case of the unsymmetrical bond, the O<sub>2</sub>-D distance was set in accord with the correlation between O<sub>2</sub>-H distance and O<sub>1</sub>...O<sub>2</sub> distance, based on neutron diffraction results. Both asymmetric and symmetric ( $R(O_1 \cdots D) = R(O_2 \cdots D)$ ) hydrogen-bonding arrangements were studied.

for the combined formaldehyde-water system were obtained for a variety of O...O distances, keeping  $\theta = 180^\circ$ . The O<sub>2</sub>-D distance was set in each case to correspond to the value empirically related to the O...O distance on the basis of a number of neutron diffraction studies.<sup>24,25</sup>

The effect of nonlinearity in the O-H...O system was investigated by performing calculations for geometries corresponding to  $\theta$  values in the range 150 to 210°, for fixed values of O<sub>1</sub>...D and O<sub>2</sub>-D, of 1.458 and 1.079 Å, respectively. The anti geometry was assumed. In addition, calculations were performed for the anti configuration,  $\theta = 180^\circ$ , for several O...O distances in the range 2.4 to 2.8 Å. In all cases zero-point vibrational amplitude effects were ignored. While this may be a minor source of error for the <sup>2</sup>H calculations, it is unlikely that it makes a significant difference in calculating the efg for <sup>17</sup>O.<sup>26</sup>

### Results

The molecular orbital (MO) calculations were carried out using one of two MO programs, both closely similar to POLYATOM.<sup>27</sup> The MO calculations were first carried out on the separated formaldehyde and water molecules, using various basis sets, and the expectation values of the efg tensor components evaluated for each case. The resultant values of  $e^2Qq_{zz}/h$  and  $\eta$  are listed in Table I. Note that the (3s2p/2s) basis set gives results nearly identical with those using the (4s2p/2s) basis set. The former set is, of course, simpler and faster to use. Addition of d functions on carbon and oxygen, and of p functions on the hydrogen atoms, results in a distinct improvement in the agreement between calculated and observed efg components. Although the discrepancy with experimental values is still substantial, it must be kept in mind that these calculations do not include corrections for Sternheimer effects, which would result in a somewhat lowered value.<sup>4</sup>

(16) Slichter, C. P. "Principles of Magnetic Resonance", 2nd ed.; Springer-Verlag: New York, 1978; p 287.

(17) Reid, R. V., Jr.; Vaida, M. L. *Phys. Rev. Lett.* **1975**, *34*, 1064.

(18) Schaefer, H. F., III; Klemm, R. A.; Harris, F. E. *Phys. Rev.* **1969**, *181*, 137.

(19) Kern, C. W.; Karplus, M. *J. Chem. Phys.* **1965**, *42*, 1062.

(20) Barfield, M.; Gottlieb, H. P. W.; Doddrell, B. M. *J. Chem. Phys.* **1978**, *69*, 4504.

(21) Dunning, T. H., Jr.; Hay, P. J. In "Methods of Electronic Structure Theory"; Schaefer, H. F., III, Eds.; Plenum Press: New York, 1977.

(22) Neumann, D.; Moskowitz, J. W. *J. Chem. Phys.* **1968**, *49*, 2056.

(23) Snyder, L. C.; Basch, H. "Molecular Wave Functions and Properties"; Wiley: New York, 1972.

(24) Olovsson, J.; Jönsson, P.-G. In ref 3, Vol. 2, p 393.

(25) Ichikawa, M. *Acta Crystallogr., Sect. B* **1978**, *34*, 2074.

(26) Kern, C. W.; Matcha, R. L. *J. Chem. Phys.* **1968**, *49*, 2081.

(27) Moskowitz, J. W.; Snyder, L. C. In "Methods of Electronic Structure Theory"; Schaefer, H. F., III, Ed.; Plenum Press: New York, 1977; Chapter 10.

Table II.  $^{17}\text{O}$  NQR Data for Hydrogen-Bonded Singly Connected Oxygen

compound	$e^2Qq_{zz}/h$	$\eta$	ref	O...O(17)	ref	ref compd	$-\Delta(e^2Qq_{zz}/h)$
1. 2-hydroxybenzaldehyde	9.891 (4)	0.282 (4)	34	2.68	63	A	0.76
2. 3-hydroxybenzaldehyde	9.923 (8)	0.318 (5)	34	2.7	<i>b</i>	A	0.72
3. 4-hydroxybenzaldehyde	9.681 (2)	0.206 (2)	34	2.684	64	A	0.97
4. 2-nitrobenzoic acid	7.602 (5)	0.306 (6)	34	2.65	65	B	1.24
5. 1,4-dihydroxyanthraquinone	9.695 (2)	0.189 (3)	34	2.576	40	C	1.02
6. chloranilic acid	10.224 (2)	0.308 (2)	34	2.769 (4)	66	D	1.01
7. 1-hydroxy-9-fluorenone	9.888 (16)	0.286 (15)	34	2.8 <sup>b</sup>	<i>b</i>	E	0.52
8. 2-nitrophenol	12.059 (1)	0.835 (2)	34	2.587 (6) <sup>c</sup>	67	F	1.15
9. 3-nitrophenol	12.292 (2)	0.714 (1)	34	2.941	68	G	0.90
10. 4-nitrophenol	12.072 (3)	0.796 (2)	34	2.818	69	H	0.97
11. 4-nitroaniline	12.57	0.743	35	3.07, 3.14	38	I	0.52
12. phthalimide	8.807 (3)	0.000 (1)	15	2.895	37	J	0.65
13. 1,8-dihydroxyanthraquinone	8.653 (2)	0.038 (1)	34	2.44, 2.54	39	C	2.06
14. salicylic acid	7.045 (3)	0.305 (4)	34	2.608, 2.636	70	B	1.80

<sup>a</sup> MHz. <sup>b</sup> Estimated O...O distance from <sup>2</sup>H NQR; see ref 61. <sup>c</sup> Assumed to be the same as that for 2-nitro-4-chlorophenol.

The dependence of the calculated efg parameters on the choice of basis set has been studied previously.<sup>19</sup> While it is true that a larger basis set leads to improved results, it is not evident that the convergence toward agreement with experimental values is monotonic. In the present work we are concerned with the differences in expectation values for the field gradient operators as the hydrogen-bonding interaction between formaldehyde is varied. These differences should be adequately reflected in the calculations employing a smaller basis set. In this connection, Allen has recently discussed the adequacy of the 4-31G basis set,<sup>28,29</sup> which is somewhat similar to the (3s2p/2s) Gaussian set employed in this work,<sup>30</sup> for the study of hydrogen-bonding interactions. He finds that while it leads to overestimation of the hydrogen-bonding energies, it gives satisfactory results for minimum-energy geometries. A similar conclusion was reached by Kollman.<sup>31</sup>

**Singly Connected Oxygen.** The orientation of the calculated principal axis system for the carbonyl oxygen, shown by the capital letters in Figure 1, is in agreement with the experimentally determined values for gaseous formaldehyde.<sup>32</sup> Using the Townes-Dailey model,<sup>33</sup> the  $^{17}\text{O}$  NQR data for a wide range of singly connected oxygen functions have been analyzed to deduce the orientations of the principal axes, based on relative populations of the  $\sigma$  and  $\pi$  orbitals.<sup>7,15,34,35</sup> For both carbonyl and nitro group oxygens, the major principal axis, i.e., the Z axis of the efg tensor, is oriented along the molecular y axis, as illustrated in Figure 1. Interchange of the orientations of  $q_{XX}$  and  $q_{YY}$  can occur, depending on the details of the  $\pi$  bonding.

We are concerned in this work with the perturbing effects of hydrogen bonding on the charge distribution at various points in the hydrogen-bonding system. It is therefore appropriate to look at the change in the field gradient parameters that occurs as the hydrogen-bonding interaction comes into play. The solid line in Figure 2a shows the difference between the calculated quadrupole coupling constant for  $^{17}\text{O}$  in the hydrogen-bonded system and that for the free formaldehyde molecule, as a function of the O...O distance. Figure 2b displays as a solid line the calculated asymmetry parameter. The  $e^2Qq_{zz}/h$  and  $\eta$  functions can be double-valued, according to whether the hydrogen bond is assumed to be symmetrical or nonsymmetrical. The empirical relationship between O<sub>2</sub>-H and O...O distances that we employed in the calculations is such that the symmetrical and nonsymmetrical forms of the hydrogen bond become equivalent at an O...O distance of 2.40 Å.

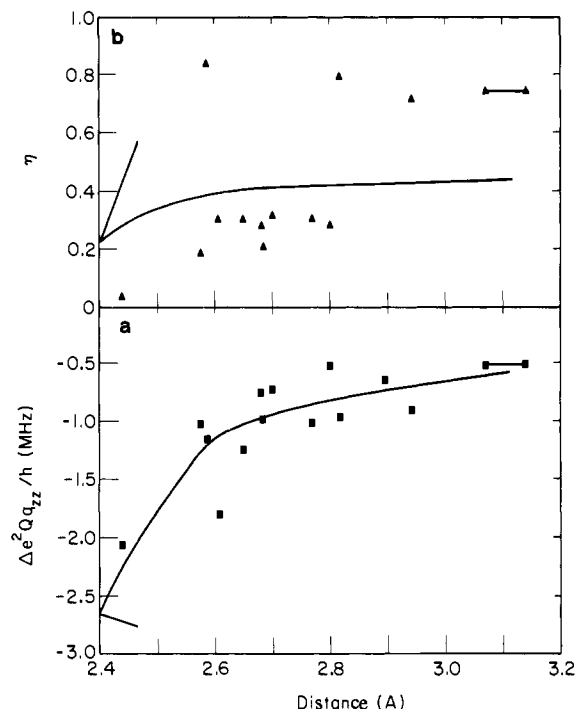


Figure 2. Calculated and experimental values of  $\Delta e^2Qq_{zz}/h$  (a) and  $\eta$  (b) as a function of O...O distance for the singly bound oxygen in O—H...O hydrogen bonding.

Table III.  $^{17}\text{O}$  NQR Data for Singly Connected, Non-Hydrogen-Bonded Reference Compounds

compound	$e^2Qq_{zz}/h$	ref
A. 4-chlorobenzaldehyde	10.648 (2)	15
B. benzyl benzoate	8.844 (8)	34
C. 1,8-dihydroxyanthraquinone	10.714 (2)	34
D. 2,5-dichlorobenzoquinone	11.258 (2)	<i>a</i>
E. 9-fluorenone	10.41 (5)	34
F. 2-nitrophenol	13.214 (2)	34
G. nitrophenol	13.197 (2)	34
H. 4-nitrophenol	13.039 (2)	34
I. nitrobenzene	13.09	35
J. phthalimide	9.455 (2)	15

<sup>a</sup> Hsieh, Y.; Koo, J. C.; Hahn, E. L. *Chem. Phys. Lett.* 1972, 13, 563.

The decrease that occurs in  $e^2Qq_{zz}/h$  for the carbonyl oxygen can be readily understood in qualitative terms by considering the orbital populations, as revealed by a Mulliken population analysis. The oxygen 2p<sub>y</sub> orbital is most extensively perturbed by the hydrogen-bonding interaction. Approach of the positive charge represented by the proton of the water O—H bond causes a radial

(28) Desmeules, P. J.; Allen, L. C. *J. Chem. Phys.* 1980, 72, 4731.

(29) Allen, L. C. *J. Am. Chem. Soc.* 1975, 97, 6921.

(30) Ditchfield, R.; Hehre, W. J.; Pople, J. A. *J. Chem. Phys.* 1971, 54, 724.

(31) Kollman, P. A. In "Applications of Electronic Structure Theory"; Schaefer, H. F., III, Ed.; Plenum Press: New York, 1977.

(32) Flygare, W. H.; Lowe, J. T. *J. Chem. Phys.* 1965, 43, 3645.

(33) Townes, C. H.; Dailey, B. P. *J. Chem. Phys.* 1949, 17, 782.

(34) Butler, L. G.; Cheng, C. P.; Brown, T. L., to be submitted for publication.

(35) Cheng, C. P.; Brown, T. L. *J. Am. Chem. Soc.* 1980, 102, 6418.

Table IV.  $^{17}\text{O}$  NQR Data for Aromatic Alcohols

compound <sup>a</sup>	$e^2Qq_{zz}/h$	$\eta$	O...O (Å)	ref
1. 2-nitrophenol	8.514 (2)	0.526 (1)	2.587 (6) <sup>a</sup>	67
2. 3-nitrophenol	8.871 (3)	0.689 (3)	2.941	68
3. 4-nitrophenol	8.607 (2)	0.620 (2)	2.818	69
4. chloranilic acid	8.359 (8)	0.415 (7)	2.769 (4)	66
5. salicylic acid	7.991 (8)	0.661 (6)	2.608	70
6. 2-hydroxybenzaldehyde	8.304 (22)	0.526 (17)	2.68	63
7. 3-hydroxybenzaldehyde	8.736 (7)	0.665 (4)	2.7	<i>b</i>
8. 4-hydroxybenzaldehyde	8.468 (3)	0.499 (2)	2.684	71
9. 1-hydroxy-9-fluorenone	8.655 (15)	0.591 (11)	2.8	<i>b</i>
10. 1,8-dihydroxyanthraquinone	8.215 (2)	0.451 (1)	2.54	39
11. 1,8-dihydroxyanthraquinone	8.121 (2)	0.469 (1)	2.44	39
12. 1,4-dihydroxyanthraquinone	8.233 (2)	0.471 (1)	2.576	40

<sup>a</sup> Assumed to be the same as that for 2-nitro-4-chlorophenol. <sup>b</sup> Estimated from  $^2\text{H}$  NQR; see ref 61.

expansion of the  $2p_y$  orbital. Because the major axis of the efg tensor lies on or near the axis of the  $2p_y$  orbital, and because the field gradient is a  $r^{-3}$  operator, eq 2, the radial expansion of the  $2p_y$  orbital results in a decrease in quadrupole coupling constant. At the same time, since the field gradient tensor is traceless, the second independent component, the asymmetry parameter, also varies.

Experimental  $^{17}\text{O}$  NQR data for singly connected oxygen functions and for a series of non-hydrogen-bonded compounds that can serve as reference compounds, are listed in Tables II and III, respectively. In choosing a suitable reference compound we assume that any changes in electronic charge distribution around the oxygen of interest, which may result from remote substituent effects or from details of the lattice arrangements, are small in comparison with the perturbing effects of the hydrogen bonding. It is evident from comparisons among the compounds in the  $^{17}\text{O}$  NQR data already collected and reported<sup>15,35,36</sup> that this is a safe assumption.

For all of the compounds listed in Table II, the  $Z$  component of the efg tensor should lie along the direction of the  $2p_y$  orbital. Thus, it is reasonable to expect that  $e^2Qq_{zz}/h$  and  $\eta$  should follow the theoretically derived relationships represented by the lines in Figure 2. The experimental values for  $e^2Qq_{zz}/h$  show remarkably good agreement with the theoretical model, considering the variety in oxygen functions among the data. Note that we are graphing the asymmetry parameter data themselves, and not changes in  $\eta$ . The data exhibit a considerable scatter; the asymmetry parameter is more sensitive to minor details of the charge distribution than is  $e^2Qq_{zz}/h$  itself. For this reason, variation in  $\eta$  is not as generally useful an index of changes in charge distribution as  $e^2Qq_{zz}/h$ .

A few of the data points in Figure 2 require discussion. Two N—H...O bonds, in phthalimide<sup>37</sup> and 4-nitroaniline,<sup>38</sup> are included. In the latter compound, there are two distinct N—H...O bonds, of lengths 3.07 and 3.14 Å, to the two nitro group oxygens. Nevertheless, only one set of  $^{17}\text{O}$  transitions was observed. In both these compounds the N...O distances are quite large, indicating that the hydrogen bonding is relatively weak. The gradient of  $e^2Qq_{zz}/h$  with O...O distance in this range of Figure 2 is quite low. Therefore, the fact that the nitrogen and oxygen atoms possess slightly different covalent radii is not a serious impediment to inclusion of these data in the correlation.

The carbonyl oxygens in salicylic acid and 1,8-dihydroxyanthraquinone are both involved in two hydrogen bonds, as illustrated in Figure 3. The two hydrogen bonds are roughly additive in their perturbing effect on  $e^2Qq_{zz}/h$  for salicylic acid, which has a much lower quadrupole coupling constant than would be expected for a single hydrogen bond with O...O distance of 2.608 Å. The data for 1,8-dihydroxyanthraquinone do not deviate from the model. However, in this case the hydrogen bonds are both short and strongly bent ( $\theta \sim 145^\circ$ ),<sup>39,40</sup> so that it is doubtful

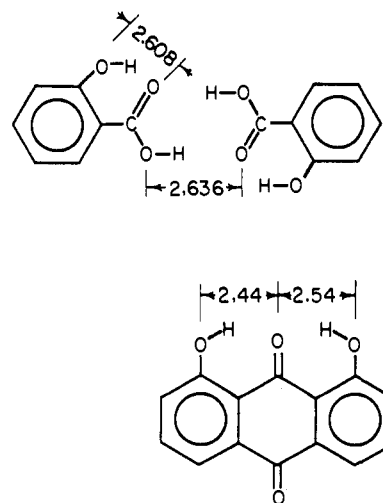


Figure 3. Geometrical arrangements of intramolecular and intermolecular hydrogen bonding in salicylic acid<sup>70</sup> and 1,8-dihydroxyanthraquinone.<sup>39</sup>

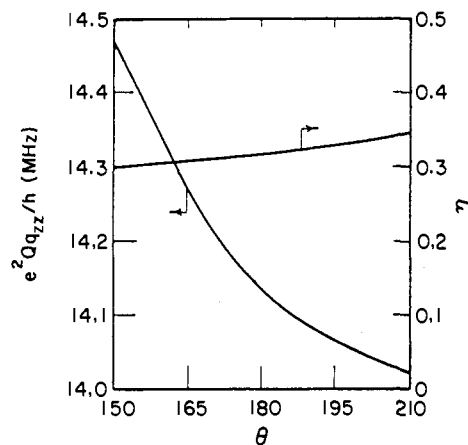


Figure 4. Calculated asymmetry parameter and quadrupole coupling constant at carbonyl oxygen as a function of angle  $\theta$  (Figure 1).

that the compound is a suitable candidate for the correlation.

The calculated field gradient parameters at the carbonyl oxygen are not much different for the syn and anti forms of the formaldehyde-water pair. The value of  $e^2Qq_{zz}/h$  for the syn form is about 0.05 MHz larger than for the anti form over the range of O...O distances 2.7 to 2.4 Å. The asymmetry parameter for the syn form is at most about 0.03 larger than for the anti form. By contrast, the effect of a change in the angle is considerable. Figure 4 shows the variation in the efg parameters as  $\theta$  (in the

(36) Hiyama, Y.; Brown, T. L. to be submitted for publication.

(37) Matzat, Von E. *Acta Crystallogr., Sect. B* 1972, 28, 415.

(38) Trueblood, K. N.; Goldish, E.; Donohue, J. *Acta Crystallogr.* 1961, 14, 1009.

(39) Prakash, A. Z. *Kristallogr., kristallogom. Kristallphys. Kristallchem.* 1965, 122, 5272.

(40) Nigam, G. D.; Deppisch, B. Z. *Kristallogr., Kristallogom. Kristallphys. Kristallchem.* 1980, 151, 185.

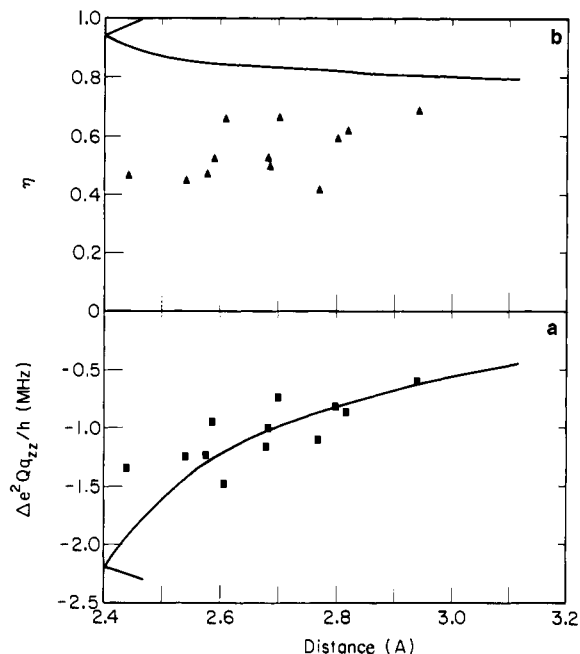


**Figure 5.** Calculated and experimental values of  $\Delta e^2Qq_{zz}/h$  (a) and  $\eta$  (b) as a function of O...O distance for the  $^{17}\text{O}$  of hydrogen-bonding OH. The experimental data are all for aromatic alcohols. The reference value for a non-hydrogen-bonding OH was chosen to provide a best fit of all the experimental data with the calculated curve.

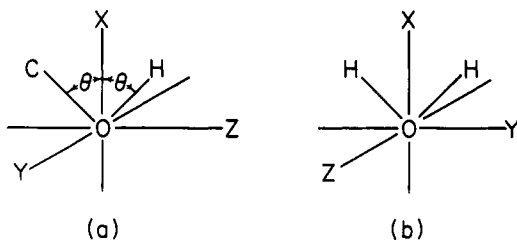


**Figure 6.** Observed orientations of the efg tensor axes at  $^{17}\text{O}$  in ethanediol (a) and in gaseous water (b). In both cases the COH or HOH atom sets lie in the plane of the paper.

anti form) is varied from 150 to 210°. Although  $\eta$  does not change significantly,  $e^2Qq_{zz}/h$  varies by about 0.4 MHz. This suggests that the correlation depicted in Figure 2a might not be particularly well obeyed for strongly bent hydrogen bonds.

**Hydroxyl Oxygen.** The oxygen atom of the water molecule in our calculations serves as a model for hydroxyl-type oxygen in hydrogen bonding of alcohols and other O–H functional groups. Figure 5 shows the manner in  $\Delta e^2Qq_{zz}/h$  and asymmetry parameter for the  $^{17}\text{O}$  of water vary as a function of the O...O distance in the formaldehyde–water calculations. The data points shown in Figure 5, and listed in Table IV, represent a series of hydrogen-bonded phenols. Only a single reference compound is needed, since all the compounds are phenols. However, the choice of reference compound is fraught with difficulties, because  $^{17}\text{O}$  NQR data for a phenol that is free of hydrogen-bonding effects are not available. We can, however, choose a reference value that gives us a “best fit” between the calculated and observed  $e^2Qq_{zz}/h$  and O...O. The value chosen, which leads to the distribution of data points shown in Figure 5, is 9.46 MHz. This represents the quadrupole coupling constant for a representative phenol oxygen that is free of hydrogen-bonding interaction.

The scatter in the fit of experimental data to the calculated curve of Figure 5a is no doubt due in part to various structural effects among the phenols, inasmuch as individual reference compounds were not chosen for each compound. Nevertheless, the overall fit between theoretical and experimental results is remarkably good.

There has been no report of a determination of the orientation of the  $^{17}\text{O}$  efg tensor axes for the oxygen of phenols. Microwave

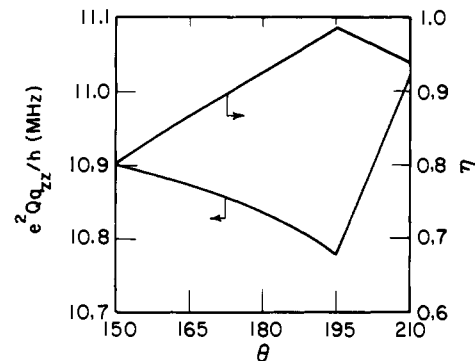


**Figure 7.** Variation in  $e^2Qq_{zz}/h$  and  $\eta$  at the oxygen of the water molecule in the water–formaldehyde pair, as a function of  $\theta$ . The discontinuity at  $\theta = 195^\circ$  represents a change in orientation of the efg tensor Z axis.

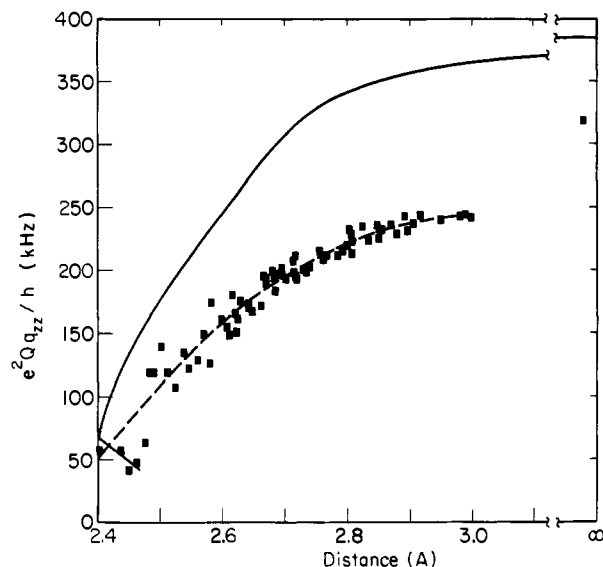


**Figure 8.** Calculated and observed variation in  $e^2Qq_{zz}/h$  for deuterium in O–H...O hydrogen bonding, as a function of O...O distance. The lower branch of the line representing the calculated results corresponds to a symmetric hydrogen bond.

spectra of gaseous  $^{17}\text{ODH}^{41}$  show that the efg tensor is oriented as shown in Figure 6b. On the other hand, for ethanediol,<sup>42</sup> the efg tensor is assigned the orientation shown in Figure 6a. Our calculations for the water–formaldehyde pair indicate that the orientation in Figure 6b, i.e., with the Z axis aligned along the normal to the molecular plane, is correct for all O...O distances greater than 2.45 Å. A similar result was obtained in connection with analysis of the  $^{17}\text{O}$  NQR data for ice Ih.<sup>43</sup>

The calculated value of  $e^2Qq_{zz}/h$  at the water oxygen was smaller by about 0.15 MHz or less for the anti form as compared with the syn, over the range of O...O distances 2.7 to 2.4 Å;  $\eta$  for the anti form was about 0.03 larger or less. The calculated variation in efg parameters with  $\theta$  (in the syn form) is illustrated in Figure 7. The discontinuity at  $\theta = 195^\circ$  is due to a change in the orientation of the major principal axis of the efg tensor, from alignment along the normal to the plane of the molecule to alignment along the x axis, as defined in Figure 6. There is no experimental evidence that such a reorientation of the efg axis occurs.

**Deuterium Quadrupole Coupling Constants.** There have been relatively few theoretical studies of field gradients at deuterium in hydrogen-bonding systems. A few hydrogen-bonding geometries

(41) Verhoeven, J.; Dymanus, A.; Bluysen, H. *J. Chem. Phys.* **1969**, *50*, 3330.

(42) Brosnan, S. G. P.; Edmonds, D. T. *J. Magn. Reson.* **1980**, *38*, 47.

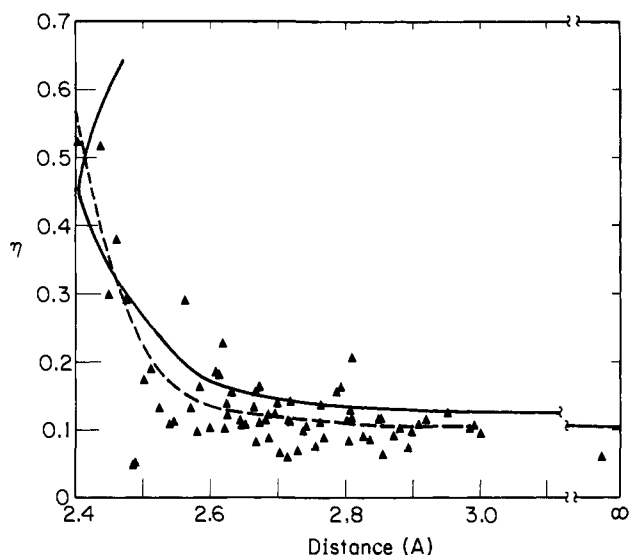
(43) Spiess, H. W.; Garrett, B. B.; Sheline, R. K.; Rabideau, S. W. *J. Chem. Phys.* **1969**, *51*, 1201.

Table V. Deuterium Quadrupole Coupling Constants and O...O Distances in O-H...O Hydrogen Bonds

	compound	$e^2Qq_{ZZ}/h$ (kHz)	$\eta$	ref	O...O dist	ref
1.	HDO	318.6 (24)	0.06 (16)	54		
2a.	CuSO <sub>4</sub> ·5H <sub>2</sub> O	241.5 (13)	0.096 (8)	10	2.999 (4)	<i>a</i>
b.		225.6 (11)	0.117 (7)		2.851 (4)	
c.		232.4 (8)	0.083 (5)		2.803 (4)	
d.		219.8 (7)	0.114 (6)		2.800 (4)	
e.		211.6 (14)	0.134 (9)		2.767 (4)	
f.		208.3 (8)	0.110 (7)		2.761 (4)	
g.		203.1 (9)	0.106 (4)		2.740 (4)	
h.		212.2 (17)	0.142 (11)		2.717 (4)	
i.		208.3 (13)	0.113 (9)		2.715 (5)	
j.		200.2 (11)	0.117 (11)		2.681 (4)	
3.	LiClO <sub>4</sub> ·3H <sub>2</sub> O	245.2 (1)	0.107 (1)	<i>b</i>	2.989 (2)	<i>c</i>
4a.	Na <sub>2</sub> S <sub>2</sub> O <sub>6</sub> ·2H <sub>2</sub> O	244.0 (30)	0.103 (3)	<i>d</i>	2.980 (15)	<i>e</i>
b.		236.0 (30)	0.116 (3)		2.848 (13)	
5a.	Li <sub>2</sub> SO <sub>4</sub> ·H <sub>2</sub> O	239.8 (11)	0.126 (7)	<i>f</i>	2.95 (1)	<i>g</i>
b.		236.6 (12)	0.091 (8)		2.87 (2)	
6.	L-serine	244.4 (1)	0.115 (3)	12	2.918 (3)	<i>h</i>
7a.	$\alpha$ -H <sub>2</sub> C <sub>2</sub> O <sub>4</sub> ·2H <sub>2</sub> O	237.2 (7)	0.108 (4)	<i>i</i>	2.906 (2)	<i>j</i>
b.		229.4 (18)	0.102 (10)		2.879 (2)	
c.		107.1 (5)	0.133 (5)		2.524 (2)	
8a.	LiHCO <sub>2</sub> ·H <sub>2</sub> O	231.3 (6)	0.097 (3)	<i>k</i>	2.896 (2)	<i>l</i>
b.		198.7 (4)	0.060 (5)		2.714 (2)	
9.	Ba(ClO <sub>3</sub> ) <sub>2</sub> ·H <sub>2</sub> O	243.5 (15)	0.074 (2)	53	2.891 (14)	<i>m</i>
10a.	$\beta$ -H <sub>2</sub> C <sub>2</sub> O <sub>4</sub> ·2H <sub>2</sub> O	232.2 (10)	0.064 (5)	<i>i</i>	2.855 (2)	<i>j</i>
b.		223.9 (8)	0.085 (5)		2.834 (3)	
10c.	$\beta$ -H <sub>2</sub> C <sub>2</sub> O <sub>4</sub> ·2H <sub>2</sub> O	134.7 (4)	0.108 (6)		2.538 (2)	
11a.	NaHC <sub>2</sub> O <sub>4</sub> ·H <sub>2</sub> O	235.2 (19)	0.09 (1)	<i>n</i>	2.824 (1)	<i>o</i>
b.		228.5 (16)	0.13 (1)		2.806 (1)	
12a.	Sr(HCOO) <sub>2</sub> ·2H <sub>2</sub> O	213.5 (4)	0.117 (3)	<i>p</i>	2.808 (7)	<i>q</i>
b.		200.7 (5)	0.098 (3)		2.736 (7)	
c.		195.7 (4)	0.116 (4)		2.715 (7)	
d.		189.3 (4)	0.110 (4)		2.672 (7)	
13a.	SnCl <sub>2</sub> ·2H <sub>2</sub> O	223.3 (4)	0.206 (3)	<i>r</i>	2.808 (4)	<i>s</i>
b.		193.2 (5)	0.112 (3)		2.718 (6)	
c.		194.2 (3)	0.066 (4)		2.702 (5)	
14.	L-hydroxyproline	214.9 (1)	0.163 (3)	12	2.792 (2)	<i>t</i>
15.	L-serine monohydrate	211.7 (1)	0.154 (3)	12	2.785 (4)	<i>u</i>
16.	(NH <sub>4</sub> ) <sub>2</sub> C <sub>2</sub> O <sub>4</sub> ·H <sub>2</sub> O	213.3 (4)	0.090 (2)	<i>v</i>	2.767 (4)	<i>w</i>
17.	K <sub>2</sub> C <sub>2</sub> O <sub>4</sub> ·H <sub>2</sub> O	216.0 (4)	0.076 (8)	<i>x</i> , 14	2.754 (2)	<i>y</i>
18a.	Te(OH) <sub>6</sub>	201.5 (1)	0.069 (2)	<i>z</i>	2.730 (2)	<i>aa</i>
b.		197.1 (1)	0.138 (2)		2.696 (2)	
c.		201.9 (1)	0.123 (2)		2.695 (2)	
d.		196.8 (1)	0.087 (2)		2.685 (2)	
19.	HIO <sub>3</sub>	184.1 (2)	0.125 (2)	<i>z</i>	2.685 (10)	<i>bb</i>
20a.	BeSO <sub>4</sub> ·4H <sub>2</sub> O	194.8 (3)	0.123 (3)	<i>f</i>	2.684 (5)	<i>cc</i>
b.		181.1 (4)	0.226 (4)		2.617 (5)	
21.	DL-serine	194.1 (1)	0.164 (3)	12	2.671 (1)	<i>u</i>
22a.	H <sub>2</sub> SeO <sub>3</sub>	196.3 (5)	0.082 (4)	<i>z</i>	2.667 (2)	<i>dd</i>
b.		165.4 (5)	0.102 (5)		2.621 (2)	
23.	L-tyrosine	193.1 (1)	0.156 (3)	12	2.666 (3)	<i>ee</i>
24.	succinic acid	172. (2)	0.134 (15)	50	2.663 (15)	<i>ff</i>
25a.	1,1-cyclobutanedicarboxylic acid	167.9 (15)	0.109 (6)	<i>gg</i>	2.649 (5)	<i>hh</i>
b.		174.1 (15)	0.109 (6)		2.644 (5)	
26a.	maleic acid	170.9 (1)	0.115 (3)	5	2.643 (2)	<i>ii</i>
b.		139.9 (1)	0.174 (3)		2.502 (2)	
27a.	KHSO <sub>4</sub>	176.0 (5)	0.156 (7)	<i>z</i>	2.630 (5)	<i>jj</i>
b.		174.4 (2)	0.164 (2)		2.583 (5)	
28.	formic acid	161.2 (1)	0.122 (1)	5	2.624 (2)	<i>kk</i>
29a.	KD <sub>3</sub> (SeO <sub>3</sub> ) <sub>2</sub>	151. (3)	0.138 (7)	<i>ll</i>	2.623 (2)	<i>mm</i>
b.		127. (3)	0.097 (5)		2.580 (2)	
30.	NaHCO <sub>3</sub>	148.8 (10)	0.182 (5)	<i>z</i>	2.611	<i>nn</i> , <i>oo</i>
31.	KHCO <sub>3</sub>	155.5 (2)	0.186 (2)	<i>pp</i>	2.607 (2)	<i>qq</i>
32a.	RbH <sub>3</sub> (SeO <sub>3</sub> ) <sub>2</sub>	161.1	0.103	<i>rr</i>	2.599 (2)	<i>ss</i>
b.		149.6	0.131		2.570 (2)	
c.		119.7	0.190		2.512 (2)	
33.	(NH <sub>4</sub> )HC <sub>2</sub> O <sub>4</sub> ·1/2H <sub>2</sub> O	129. (3)	0.29 (3)	<i>tt</i>	2.561 (2)	<i>uu</i>
34.	potassium acid phthalate	122.7 (2)	0.111 (3)	<i>vv</i>	2.546	<i>ww</i>
35.	NH <sub>4</sub> H <sub>2</sub> PO <sub>4</sub>	119.6 (8)	0.053 (8)	8	2.490 (1)	<i>xx</i>
36.	KH <sub>2</sub> PO <sub>4</sub>	119.5	0.049	59	2.487 (5)	<i>yy</i>
37.	potassium oxodiacetate	64. (2)	0.29 (2)	50	2.476 (2)	<i>zz</i>
38.	sodium oxodiacetate	48. (2)	0.38 (2)	50	2.462 (3)	<i>aa</i>
39.	rubidium oxodiacetate	41. (1)	0.30 (2)	50	2.449 (3)	<i>zz</i>
40.	potassium hydrogen maleate	57.2	0.516	<i>bbb</i>	2.437 (4)	<i>ccc</i> , <i>ddd</i>
41.	potassium hydrogen chloromaleate	57.3	0.523	<i>bbb</i>	2.403 (3)	<i>eee</i>

(Table V footnotes)

<sup>a</sup> Bacon, G. E.; TiHerton, D. H. Z. *Kristallogr. Kristallgeom. Kristallphys. Kristallchem.* 1975, 141, 330. <sup>b</sup> Berglund, B.; Tegenfeldt, J. *Acta Chem. Scand.* 1978, 32, 1. <sup>c</sup> Sequeira, A.; Bernal, I.; Brown, I. D.; Faggiani, R. *Acta Crystallogr., Sect. B* 1975, 31, 1735. <sup>d</sup> Ketudat, S.; Berthold, I.; Weiss, A. Z. *Naturforsch., Teil A* 1967, 22, 1452. <sup>e</sup> Berthold, I.; Weiss, A. *Ibid.* 1967, 22, 1440. <sup>f</sup> Berglund, B.; Tegenfeldt, J. *J. Mol. Struct.* 1977, 39, 207. <sup>g</sup> Smith, H. G.; Peterson, S. W.; Levy, H. A. *J. Chem. Soc.* 1968, 48, 5561. <sup>h</sup> Kistenmacher, T. J.; Rand, G. A.; Marsh, R. E. *Acta Crystallogr., Sect. B* 1974, 30, 2573. <sup>i</sup> Chiba, T.; Soda, G. *Bull. Chem. Soc. Jpn.* 1971, 44, 1703. <sup>j</sup> Coppens, P.; Sabine, T. M. *Acta Crystallogr., Sect. B* 1969, 25, 2442. <sup>k</sup> Berglund, B.; Lindgren, J.; Tegenfeldt, J. *J. Mol. Struct.* 1974, 21, 135. <sup>l</sup> Tellgren, R.; Ramanujam, P. S.; Liminga, R. *Ferroelectrics* 1974, 6, 191. <sup>m</sup> Sikka, S. K.; Momin, S. N.; Rajagopal, H.; Chidambaram, R. *J. Chem. Phys.* 1968, 48, 1883. <sup>n</sup> Berglund, B.; Tegenfeldt, J. *Mol. Phys.* 1973, 26, 633. <sup>o</sup> Tellgren, R.; Thomas, J. O.; Olovsson, I. *Acta Crystallogr., Sect. B* 1977, 33, 3500. <sup>p</sup> Berglund, B.; Tegenfeldt, J. Z. *Naturforsch., Teil A* 1977, 32, 1025. <sup>q</sup> Golligne, J. L. *Acta Crystallogr., Sect. B* 1971, 27, 2429. <sup>r</sup> Kiriyama, H.; Nakamura, O. *Bull. Chem. Soc. Jpn.* 1980, 53, 635. <sup>s</sup> Kitahama, K.; Kiriyama, H. *Ibid.* 1977, 50, 3167. <sup>t</sup> Koetzle, T. F.; Lehmann, M. S.; Hamilton, W. C. *Acta Crystallogr., Sect. B* 1973, 29, 231. <sup>u</sup> Frey, M. N.; Lehmann, M. S.; Koetzle, T. F.; Hamilton, W. C. *Ibid.* 1973, 29, 876. <sup>v</sup> Chiba, T. *Bull. Chem. Soc. Jpn.* 1970, 43, 1939. <sup>w</sup> Taylor, J. C.; Sabine, T. M. *Acta Crystallogr., Sect. B* 1972, 28, 3340. <sup>x</sup> Pedersen, B. *Acta Chem. Scand.* 1968, 22, 453. <sup>y</sup> Sequeira, A.; Srikanta, S.; Chidambaram, R. *Acta Crystallogr., Sect. B* 1970, 26, 77. <sup>z</sup> Poplett, J. J. F.; Smith, J. A. S. *J. Chem. Soc., Faraday Trans. 2* 1978, 74, 1077. <sup>aa</sup> Lindquist, O.; Lehmann, M. S. *Acta Chem. Scand.* 1973, 27, 85. <sup>bb</sup> Garrett, B. S. Oak Ridge National Laboratory Report 1745, 1954, p 97. <sup>cc</sup> Sikka, S. K.; Chidambaram, R. *Acta Crystallogr., Sect. B* 1969, 25, 310. <sup>dd</sup> Larsen, F. K.; Lehmann, M. S.; Stofte, I. *Acta Chem. Scand.* 1971, 25, 1233. <sup>ee</sup> Frey, M. N.; Koetzle, T. F.; Lehmann, M. S.; Hamilton, W. C. *J. Chem. Phys.* 1973, 58, 2547. <sup>ff</sup> Broadley, J. S.; Cruickshank, D. W. J.; Morrison, J. D.; Robertson, J. M.; Shearer, H. M. M. *Proc. R. Soc. London, Ser. A* 1959, 251, 441. <sup>gg</sup> Dalton, L. R.; Kwiram, A. L. *J. Am. Chem. Soc.* 1972, 94, 6930. <sup>hh</sup> Soltzberg, L.; Margulis, T. N. *J. Chem. Phys.* 1971, 35, 4907. <sup>ii</sup> James, M. N. G.; Williams, G. J. B. *Acta Crystallogr., Sect. B* 1974, 30, 1249. <sup>jj</sup> Cotton, F. A.; Frenz, B. A.; Hunter, D. L. *Ibid.* 1975, 31, 302. <sup>kk</sup> Nahringbauer, I. *Ibid.* 1978, 34, 315. <sup>ll</sup> Grande, S.; Mecke, H. D.; Shuvalov, L. A. *Phys. Status Solidi A* 1978, 46, 547. <sup>mm</sup> Lehmann, M. S.; Larsen, F. K. *Acta Chem. Scand.* 1971, 25, 3859. <sup>nn</sup> Sass, R. L.; Scheuerman, R. F. *Acta Crystallogr.* 1962, 15, 77. <sup>oo</sup> Sharma, B. D. *Ibid.* 1965, 18, 818. <sup>pp</sup> Poplett, J. J. F.; Smith, J. A. S. *J. Chem. Soc., Faraday Trans. 2* 1979, 75, 1054. <sup>qq</sup> Thomas, J. O.; Tellgren, R.; Olovsson, I. *Acta Crystallogr., Sect. B* 1974, 30, 2540. <sup>rr</sup> Sakai, A.; Kasahara, M.; Tatsuzaki, I. *J. Phys. Soc. Jpn.* 1979, 47, 161. <sup>ss</sup> Tellgren, R.; Liminga, R. *Ferroelectrics* 1977, 15, 15. <sup>tt</sup> van Willigen, H.; Haberkorn, R. A.; Griffin, R. G. *J. Chem. Phys.* 1977, 67, 917. <sup>uu</sup> Kupperts, H. *Acta Crystallogr., Sect. B* 1973, 29, 318. <sup>vv</sup> Butler, L. G.; Brown, T. L., unpublished results. <sup>ww</sup> Okaya, Y. *Acta Crystallogr.* 1965, 19, 879. <sup>xx</sup> Khan, A. A.; Baur, W. H. *Acta Crystallogr., Sect. B* 1973, 29, 2721. <sup>yy</sup> Bacon, G. E.; Pease, R. S. *Proc. R. Soc. London, Ser. A* 1955, 230, 359. <sup>zz</sup> Albertson, J.; Grenthe, I. *Acta Crystallogr., Sect. B* 1973, 29, 2751. <sup>aaa</sup> Albertson, J.; Grenthe, T. Herbertsson, H. *Ibid.* 1973, 29, 1855. <sup>bbb</sup> Poplett, J. J. F.; Smith, J. A. S. *J. Chem. Soc., Faraday Trans. 2* 1979, 75, 1703. <sup>ccc</sup> Peterson, S. W.; Levy, H. A. *J. Chem. Phys.* 1958, 29, 948. <sup>ddd</sup> Darlow, S. F.; Cochran, W. *Acta Crystallogr.* 1961, 14, 1250. <sup>eee</sup> Ellison, R. D.; Levy, H. A. *Ibid.* 1965, 19, 260.



**Figure 9.** Calculated and observed variation in  $\eta$  for deuterium in O—H...O hydrogen bonding, as a function of O...O distance. The upper branch of the curve representing the calculations corresponds to a symmetrical hydrogen bond.

have been studied for water dimers<sup>11,44-46</sup> and hydrates.<sup>47,48</sup> Semiempirical MO calculations have been used to estimate <sup>2</sup>H coupling constants for maleate,<sup>49,50</sup> monoprotonated trifluoroacetic acid anion dimer,<sup>49</sup> and succinic acid.<sup>50</sup> Malondialdehyde has been studied via ab initio methods employing extended basis sets at the SCF and CI levels.<sup>51,52</sup>

The calculated field gradients at the hydrogen-bonding deuterium in the formaldehyde-water pair as a function of the O...O distance is shown as the solid line in Figure 8. The corresponding graph for  $\eta$  is shown in Figure 9. The data points on the figure represent a compilation of the substantial body of literature data regarding  $e^2Qq_{zz}/h$  and (less frequently)  $\eta$  for hydrogen-bonded systems (Table V). We have restricted the data chosen to those cases for which accurate structural information is available. No account was taken of isotope effects on the O...O distance in the deuterated species, as opposed to the protonated species on which the structures are for the most part carried out. The distance changes are expected to be on the order of 0.02 Å,<sup>2,24</sup> not a significant difference for our purposes. As an additional restriction, we have considered only hydrogen-bonding geometries which are within 30° of linearity.

The experimental values of  $e^2Qq_{zz}/h$  for <sup>2</sup>H in asymmetric hydrogen bonds were fitted with the following equation:

$$e^2Qq_{zz}/h = 5414.7 + 4113.7R_{O...O} - 857.02R_{O...O}^2 + 38.146R_{O...O}^3$$

The asymmetry parameter for asymmetric hydrogen bonds were fitted with the following equation:

$$\eta = 10144.342 - 18198.0377R_{O...O} + 13051.9849R_{O...O}^2 - 4678.13754R_{O...O}^3 + 837.92196R_{O...O}^4 - 59.99982R_{O...O}^5$$

The theoretical model leads to a dependence of  $e^2Qq_{zz}/h$  upon O...O distance that is remarkably similar to that found experimentally. We have not made any attempt to scale the theoretical results to fit the experimental results for the free water molecule. If we had done that, the agreement with experiment would have been even closer. Because the functional form of the dependence of field gradient on O...O distance is so well represented by the model, we can confidently examine the calculations to look for the origins of the marked decrease in quadrupole coupling constant with increasing hydrogen-bond strength.

(44) Weissmann, M. *J. Chem. Phys.* 1966, 44, 422.  
 (45) Olympia, P. L., Jr.; Fung, B. M. *J. Chem. Phys.* 1969, 51, 2976.  
 (46) Gornostansky, S. D.; Kern, C. W. *J. Chem. Phys.* 1971, 55, 3253.  
 (47) Almlöf, J.; Lindgren, J.; Tegenfeldt, J. *J. Mol. Struct.* 1972, 14, 427.  
 (48) Lindgren, J.; Tegenfeldt, J. *J. Mol. Struct.* 1974, 20, 335.  
 (49) Zaucer, M.; Zakrajsek, E.; Koller, J.; Hadži, D.; Azman, A. *Mol. Phys.* 1971, 21, 461.  
 (50) Mayas, L.; Plato, M.; Winscom, C. J.; Möbius, K. *Mol. Phys.* 1978, 36, 753.

(51) Karlström, G.; Wennerström, H.; Jönsson, B.; Forsén, S.; Almlöf, J.; Roos, B. *J. Am. Chem. Soc.* 1975, 97, 4188.  
 (52) Karlström, G.; Jönsson, B.; Roos, B.; Wennerström, H. *J. Am. Chem. Soc.* 1976, 98, 6851.

It has been known for a long time that the  $^2\text{H}$  quadrupole coupling constant decreases markedly upon hydrogen-bond formation, not only in  $\text{O}-\text{H}\cdots\text{O}$  hydrogen bonds, but in  $\text{N}-\text{H}\cdots\text{N}$  and other types as well.<sup>8-14,53</sup> The calculations show that the  $Z$  axis of the deuterium efg tensor at deuterium lies along the  $\text{O}-\text{H}\cdots\text{O}$  internuclear vector, and that the  $Y$  axis lies normal to the plane of the water molecule, in agreement with experimental results.<sup>54</sup> In assessing the significance of the quadrupole coupling constant data, one must keep in mind that the electronic contribution to the field gradient at deuterium arises almost entirely from centers other than the deuterium itself, because the  $1s$  orbital at the deuterium makes no contribution. The field gradient at deuterium in the free water molecule can be ascribed entirely to a net positive charge resident at the oxygen atom. When hydrogen bonding sets in, the  $\text{O}-\text{H}$  bond length increases, in accordance with a well-established empirical relationship between  $\text{O}-\text{H}$  and the  $\text{O}\cdots\text{O}$  distance.<sup>24,25</sup> Because of the steep  $r^{-3}$  dependence of the field gradient on distance, the small lengthening of the  $\text{O}_2-\text{H}$  bond (Figure 1) has a greater effect on lowering the deuterium field gradient than the new, but more distant charge distribution represented by  $\text{O}_1$ .

It has been argued<sup>8</sup> that if the  $\text{OH}$  bond distance were to increase to about 1.3 to 1.4 Å, the electronic contribution to the field gradient would begin to dominate, with a resultant change in the sign of the quadrupole coupling constant. In such a case, if we can assume for the moment that the efg tensor at deuterium is axially symmetric ( $\eta = 0$ ), the quadrupole coupling constant would have decreased to a value of zero and then begun to increase. In practice, we find small, nonzero values for  $\eta$  in  $\text{O}-\text{H}$  bonds. When there is some small departure from axial symmetry,  $e^2Qq_{zz}$  decreases with increasing  $\text{O}-\text{H}$  distance until  $q_{zz}$  is equal to  $q_{yy}$ . At this point ( $\eta = 1$ ), the quadrupole coupling constant has some relatively small value. Still further increase in the  $\text{O}-\text{H}$  distance may cause the field gradient component along the  $\text{O}-\text{H}$  bond to again have the largest value, so that the  $Z$  axis of the efg tensor lies more or less along the  $\text{O}-\text{H}$  bond, but  $e^2Qq_{zz}$  is of opposite sign.

A calculation for an assumed symmetrical hydrogen-bond form of malondialdehyde, with  $\text{O}-\text{H}$  distances of 1.18 Å, and  $\theta = 158.8^\circ$ , yielded an orientation of the  $Z$  component in the plane bisecting the  $\text{OHO}$  angle, and normal to the molecular plane.<sup>51</sup> The sign of the quadrupole coupling constant in this case remains positive. The possibility of a negative quadrupole coupling constant at deuterium was mentioned for the case of  $\text{FDF}^-$  by Kern and Karpus,<sup>19</sup> and investigated further by Dixon and co-workers.<sup>55</sup> Calculations with extended basis sets indicated a small but positive coupling constant for the symmetric hydrogen bond with a  $\text{F}\cdots\text{F}$  distance of 2.277 Å which corresponds to the observed distance in  $\text{KHF}_2$ .<sup>56,57</sup> The experimentally determined quadrupole coupling constant<sup>58</sup> is  $58 \pm 10$  kHz, with  $\eta = 0.4 \pm 0.1$ , in good agreement with the theoretical expectations. However, the calculations lead to the conclusion that for a symmetric hydrogen bond, with a larger  $\text{F}\cdots\text{F}$  distance of 2.38 Å, the deuterium quadrupole coupling constant would be negative.<sup>55</sup>

In the linear hydrogen-bonding model for which we have done calculations, the major axis of the efg tensor remains more or less along the  $\text{O}-\text{H}\cdots\text{O}$  axis, and  $e^2Qq_{zz}/h$  is positive, for all values of  $\text{O}\cdots\text{O}$ . Note, however, in Figure 8 that  $e^2Qq_{zz}/h$  is lower for the branch corresponding to an assumed symmetric hydrogen bond. Similarly, for the same  $\text{O}\cdots\text{O}$  distance,  $\eta$  is larger for the symmetric hydrogen-bond case as compared with the unsymmetric. Although we have not extended the calculations to this regime, it would appear that for an  $\text{O}\cdots\text{O}$  distance on the order of 2.6 Å

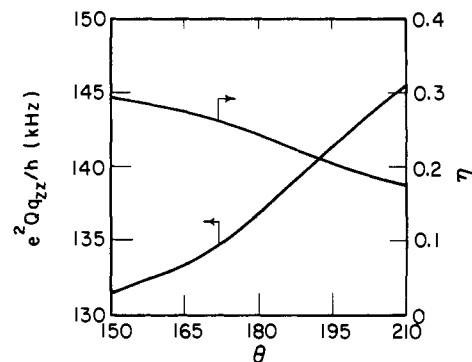


Figure 10. Variation in  $e^2Qq_{zz}/h$  and  $\eta$  for  $^2\text{H}$  in the water-formaldehyde pair as a function of  $\theta$ .

a symmetric hydrogen bond would produce a change in orientation of the  $Z$  axis. However, all of the experimental data available are in good agreement with the calculations for an unsymmetric or short symmetric hydrogen bond, which leads in all cases to an alignment of the  $Z$  axis of the deuterium efg tensor more or less along the  $\text{O}-\text{H}\cdots\text{O}$  axis, and to a positive sign for  $e^2Qq_{zz}/h$ . There is not at present any convincing basis for assigning a negative sign to the quadrupole coupling constant at deuterium in any  $\text{O}-\text{H}\cdots\text{O}$  hydrogen bond.

The efg tensor at deuterium is not at all sensitive to a change from syn to anti geometry. Departure from linearity produces a modest change in both  $e^2Qq_{zz}/h$  and  $\eta$ , as illustrated in Figure 10. (As noted above, the calculations relating to the effects of bending were carried out using the anti geometry.)

It is of interest that the  $^2\text{H}$  data for phosphates (Table V) exhibit what appears to be an anomalously low value of  $\eta$  for a given  $\text{O}\cdots\text{O}$  distance. The data shown for  $\text{ND}_2\text{D}_2\text{PO}_4$  and  $\text{KD}_2\text{PO}_4$ , taken at room temperature,<sup>8,59</sup> correspond to the dynamically disordered, nonpyroelectric phases of these substances. This choice was made because accurate structures are not available for the low-temperature pyroelectric phases. However, it has been reported that for  $\text{KD}_2\text{PO}_4$  at 173 K,<sup>60</sup> below the phase transition temperature,  $e^2Qq_{zz}/h$  is only 8 kHz higher than at 303 K, and  $\eta$  is still anomalously low, only about 0.115. It would thus appear that even in the low-temperature phase the deuterium jump frequency may be in the fast-exchange regime with respect to the NQR experiment.

The work reported here has led to the first reported theoretical and empirical correlation of  $^{17}\text{O}$  NQR data with hydrogen-bonding geometry at both the donor and acceptor atom sites. Further, we have extended the analysis of  $^2\text{H}$  NQR data, and have compiled a master correlation of  $e^2Qq_{zz}/h$  and  $\eta$  as a function of  $\text{O}\cdots\text{O}$  distance for  $^2\text{H}$ . These results make it possible to assign  $\text{O}\cdots\text{O}$  distances with good accuracy in solid-state hydrogen bonds, and they provide a detailed picture of the redistribution in electronic charge that accompanies hydrogen bonding. Our results show

(53) Chiba, T. *J. Chem. Phys.* **1963**, *39*, 947.

(54) Thaddeus, P.; Krisher, L. C.; Loubser, J. H. N. *J. Chem. Phys.* **1964**, *40*, 257.

(55) Dixon, M.; Overill, R. E.; Platt, E. *J. Mol. Struct.* **1978**, *48*, 115.

(56) Ibers, J. A. *J. Chem. Phys.* **1964**, *40*, 402.

(57) Chebotaryov, A. N.; Ludman, C. J.; Waddington, T. C.; Pang, E. K. C.; Smith, J. A. S. *J. Chem. Soc., Faraday Trans. 2* **1975**, *75*, 1565.

(58) Blinc, R.; Rutar, V.; Seliger, J.; Slak, J.; Smolej, V. *Chem. Phys. Lett.* **1977**, *48*, 576.

(59) Bjorkstam, J. L.; Uehling, E. A. *Phys. Rev.* **1959**, *114*, 961.

(60) Blinc, R.; Stepišnik, J.; Jamšek-Vilfan, M.; Žumer, S. *J. Chem. Phys.* **1971**, *54*, 187.

(61) Butler, L. G.; Hiyama, Y.; Brown, T. L., in preparation.

(62) Neumann, D. B.; Moskowitz, J. W. *J. Chem. Phys.* **1969**, *50*, 2216.

(63) Bourre-Maladière, P. C. R. *Acad. Sci.* **1953**, *237*, 825.

(64) Iwasaki, F. *Acta Crystallogr., Sect. B* **1977**, *33*, 1646.

(65) Tavale, S. S.; Pont, L. M. *Acta Crystallogr., Sect. B* **1973**, *29*, 2979.

(66) Andersen, E. K. *Acta Crystallogr.* **1967**, *22*, 188.

(67) Kawai, R.; Kashino, S.; Haisa, M. *Acta Crystallogr., Sect. B* **1976**, *32*, 1972.

(68) Pandarese, F.; Ungaretti, L.; Coda, A. *Acta Crystallogr., Sect. B* **1975**, *31*, 2671.

(69) Coppens, P.; Schmidt, G. M. J. *Acta Crystallogr.* **1965**, *18*, 62.

(70) Bacon, G. E.; Jude, R. J. Z. *Kristallogr., Kristallgeom. Kristallphys. Kristallchem.* **1973**, *138*, S19.

(71) Iwasaki, F. *Acta Crystallogr., Sect. B* **1977**, *33*, 1646.

(72) Note Added in Proof: J. E. Gready has recently published a theoretical treatment of hydrogen bonding in formic acid. Gready, J. E. *Chem. Phys.* **1981**, *55*, 1-26.



that marked departure from linearity in the hydrogen bond produces a significant change in efg parameters, particularly at deuterium. In a subsequent paper we will present experimental results that relate to strongly bent intramolecular hydrogen bonds.<sup>61</sup>

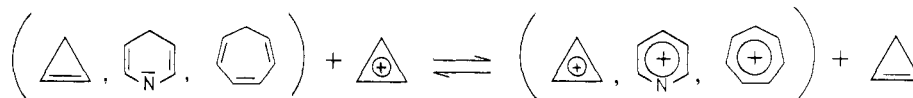
**Acknowledgment.** This research was supported by the National Science Foundation through Research Grant DMR-77-23999, with the Materials Research Laboratory, University of Illinois. We are indebted to A. B. Kunz, H. Itoh, and C. E. Dykstra for assistance in setting up the molecular orbital calculations.

## The Hydride-Donation Reaction of Reduced Nicotinamide Adenine Dinucleotide. 1. MINDO/3 and STO-3G Calculations on Analogue Reactions with Cyclopropene, Tropilidene, and 1,4-Dihydropyridine as Hydride Donors and the Cyclopropenium Cation as Acceptor

M. C. A. Donkersloot\* and H. M. Buck

Contribution from the Department of Organic Chemistry, Eindhoven University of Technology, Eindhoven, The Netherlands. Received December 2, 1980

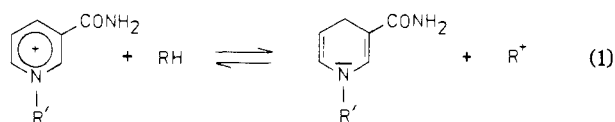
**Abstract:** On the basis of MO arguments it is made plausible that the hydride-transfer reactions are valid and useful analogues



of the NAD<sup>+</sup>/NADH hydride-transfer reaction. By means of MINDO/3-enthalpy contour maps a suitable reaction coordinate is found for each reaction. For the simplest system cyclopropene/cyclopropenium cation, the enthalpy profile along the reaction coordinate is compared with ab initio (STO-3G) results. It is demonstrated that both methods produce very similar results with regard to the overall course of the reaction (the reaction pathway), but that MINDO/3 yields a much lower activation enthalpy than STO-3G. The results indicate that the studied hydride-transfer reactions can all be conveniently described with reference to a supermolecule of C<sub>3</sub> symmetry, containing a linear C...H...C fragment. The reaction consists of a concerted and gradual breaking of one, and forming of the other one of the C-H bonds in this fragment. Simultaneously transfer of negative charge takes place, the overall result being the migration of a hydride ion.

### Introduction

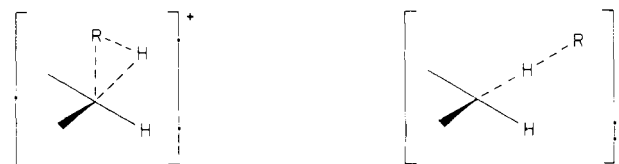
During recent years the coenzyme nicotinamide adenine dinucleotide (NAD<sup>+</sup>) has received widespread attention. This coenzyme plays an important role in a large number of enzyme-catalyzed oxidation-reduction reactions.<sup>1</sup> The characteristic event in these reactions is always the reversible transfer of a hydride ion from the substrate to the 4 position of the nicotinamide moiety of NAD<sup>+</sup> or vice versa:



where RH = a suitable hydride donor

Much work has been done to elucidate the reaction mechanism of this process. In particular, kinetic studies on NAD<sup>+</sup>/NADH as well as on a variety of model compounds—with or without enzymatic catalysis—contributed to our understanding of the hydride-transfer reaction. However, up to now it has not been possible to combine all results in one simple overall scheme. We refer, for instance, to two recent studies on nonenzymatic hydride-transfer model reactions, leading to quite different conclusions. Van Eikeren et al.<sup>2</sup> studied the hydride transfer between *N*-benzyl-3-carbamoyl-1,4-dihydropyridine and the *N*-benzyl-3-

carbamoylpyridinium cation. On the basis of their results they proposed a mechanism involving an intermediate radical-cation-radical pair, formed by the initial transfer of an electron. On the other hand, Kurz and Frieden<sup>3</sup> studied the reductive desulfonation of 4-cyano-2,6-dinitrobenzenesulfonates with dihydronicotinamide and reached the conclusion that this reaction occurs by direct hydride-ion transfer with the transfer of negative charge and of the hydrogen nucleus taking place in a single kinetic event. In addition to this ambiguity with respect to the identity of the migrating moiety there is also an uncertainty as regards the structure of the transition state. A triangular arrangement was proposed by Lewis and Symons,<sup>4</sup> whereas Swain et al.<sup>5</sup> advocated a linear transition state:



Finally, a very typical and as yet not fully understood feature of the NAD<sup>+</sup>/NADH hydride-transfer reaction is its stereospecificity under enzymatic conditions, demonstrated by Vennesland and Westheimer.<sup>6</sup> In this and the subsequent paper we endeavor to elucidate the nature of the NAD<sup>+</sup>/NADH hydride-transfer re-

(1) Sund, H. "Pyridine Nucleotide-Dependent Dehydrogenases"; W. de Gruyter & Co.: Berlin, West Germany.

(2) Van Eikeren, P.; Kenney, P.; Tokmakian, R. *J. Am. Chem. Soc.* **1979**, *101*, 7402-7406.

(3) Kurz, L. C.; Frieden, C. *J. Am. Chem. Soc.* **1980**, *102*, 4198-4203.

(4) Lewis, E. S.; Symons, M. C. R. *Q. Rev. Chem. Soc.* **1958**, *12*, 230-249.

(5) Swain, C. G.; Wiles, R. A.; Bader, R. F. W. *J. Am. Chem. Soc.* **1961**, *83*, 1945-1950.

(6) Vennesland, B.; Westheimer, F. H. In "The Mechanism of Enzyme Action"; McElroy, W. D.; Glass, B., Eds.; John Hopkins Press: Baltimore, 1954.